

## Excitons in motion in II–VI semiconductors

J. J. Davies\*<sup>1</sup>, L. C. Smith<sup>1</sup>, D. Wolverson<sup>1</sup>, V. P. Kochereshko<sup>2</sup>, J. Cibert<sup>3</sup>, H. Mariette<sup>3</sup>, H. Boukari<sup>3</sup>, M. Wiater<sup>4</sup>, G. Karczewski<sup>4</sup>, T. Wojtowicz<sup>4</sup>, A. Gust<sup>5</sup>, C. Kruse<sup>5</sup>, and D. Hommel<sup>5</sup>

Received 4 September 2009, revised 13 October 2009, accepted 25 October 2009 Published online 2 April 2010

Keywords II-VI semiconductors, excitons, photoluminescence

We have shown recently that the magnetic properties of excitons change significantly as the excitons acquire kinetic energy. In particular, the exciton magnetic moments are enhanced considerably, whilst the diamagnetism decreases. The behaviour can be investigated through spectroscopic studies of excitons confined in quantum wells of large width (greater than five times the exciton Bohr radius) and these motion-induced changes in the magnetic properties have now been observed for CdTe, ZnSe, ZnTe and GaAs. The present

paper summarises these phenomena, with particular focus on CdTe and ZnSe, and shows that the changes can be accounted for by motion-induced mixing between the exciton ground and higher lying states. The mixing is caused by the  $\gamma_3$  term in the Luttinger Hamiltonian which describes the dispersion curves for the valence band and, as a result, the form of the exciton wavefunction becomes motion-dependent. For both materials, excellent agreement is obtained between experiment and the results predicted by this mechanism.

© 2010 WILEY-VCH Verlag GmbH & Co. KGaA, Weinheim

**1 Introduction** What happens to excitons when they move through semiconductors? To answer this question is not easy, since the usual method of investigating the structure of excitons is to use optical spectroscopy and, unfortunately, the small wavevector of photons means that only excitons with low values of their translational wavevectors can conventionally be studied. To overcome this difficulty, we have in a series of recent investigations [1–6] studied excitons in potential wells which are sufficiently wide for quantum confinement energies to be smaller than the exciton binding energy. In such quantum wells, the exciton can be described in the adiabatic or centre of mass (CoM) approximation [7, 8], in which it is considered as a composite particle formed from the electron and the hole mutually orbiting each other. The translational wavevector  $K_7$  of the exciton as a whole is then quantised approximately according to  $K_z = n\pi/L$ , where L is the width of the quantum well and N is a non-zero integer, and the recombination transition energies of the exciton then have discrete values. As a result of the loss in translational symmetry, photons can interact with excitons with large values of  $K_z$  and the transition associated with each value of  $K_z$  can be studied individually. We have used this approach to investigate how each transition behaves when a magnetic field is applied and shown that the magnetic properties of the exciton change markedly as it acquires kinetic energy.

To account for these properties we have proposed a model [2] which involves motion-induced mixing between the exciton ground state (which has a 1S envelope function) and higher lying nP states. The source of the mixing involves the  $\gamma_3$  terms in the description of the dispersion curves for the valence band. The model provides a successful quantitative description of motion-induced changes in the magnetic moments and in the diamagnetism of excitons in CdTe. The purpose of the present paper is to review this model and to show that it provides an excellent description not only for CdTe but also for ZnSe [6], suggesting that it is universally applicable to excitons in all zinc-blende semiconductors. Similar effects have been observed for GaAs [1].

The plan of the paper is as follows. In Section 2–4 we describe representative data for CoM excitons under



<sup>&</sup>lt;sup>1</sup>Department of Physics, University of Bath, Bath BA2 7AY, UK

<sup>&</sup>lt;sup>2</sup> A.F. Ioffe Physico-Technical Institute, RAS, 194021 St. Petersburg, Russia

<sup>&</sup>lt;sup>3</sup> Institut Néel, CNRS-Université Joseph Fourier, 38042 Grenoble Cedex 9, France

<sup>&</sup>lt;sup>4</sup>Institute of Physics, Polish Academy of Sciences, 02-668 Warsaw, Poland

<sup>&</sup>lt;sup>5</sup> Institute for Solid State Physics, Semiconductor Epitaxy Group, University of Bremen, 28334 Bremen, Germany

<sup>\*</sup>Corresponding author: e-mail j.j.davies@bath.ac.uk, Phone: +44 1225 383324, Fax: +44 1225 386110



magnetic fields in CdTe and in ZnSe, followed in Section 5 by a description of the key features of the motion-induced mixing process. In Section 6 we discuss application to CdTe and to ZnSe and show that excellent agreement with the experimental data is obtained by using valence band parameters which are close to those obtained independently.

**2 Experimental details** The specimens studied were all grown by molecular beam epitaxy as described in Refs. [2, 9]. The CdTe and ZnSe wells were strained, with the energies of the heavy hole states being lower than those of the light hole states. All specimens discussed in the present paper were grown on (001) substrates.

Photoluminescence (PL), transmission, reflectivity and PL excitation (PLE) spectra were recorded with the specimens at low temperature (2–26 K) in magnetic fields up to 8 T. Experiments could be carried out with the field parallel to or perpendicular to the quantum well growth direction and also at intermediate orientations.

**3 Excitons in wide quantum wells** Most of the quantum wells which we shall discuss have widths which are more than five times the exciton Bohr radius ( $a_{\rm exc}$ ). If the quantum wells were infinitely deep, the energies of photons emitted during the recombination in states of a particular value of N would be given by:

$$E_{\rm N} = E_0 + \frac{N^2 h^2}{8ML^2},\tag{1}$$

where M is the exciton translational mass for motion in the growth direction and where  $E_0$  is the exciton recombination energy in a well of infinite width. The states of different N can therefore be observed in absorption, reflectivity, PL and PLE spectra. Examples of PLE spectra for a CdTe quantum well are shown in Fig. 1, in which a series of clearly resolved signals corresponding to different values of N are observed. If the transition energies are plotted against  $(N/L)^2$  with the correct choices for N, they should lie on a straight line given by Eq. (1). Figure 2 shows such plots for CdTe and ZnSe, confirming the identification of the indices (and hence the values of  $K_2$ ) assigned to each transition (see also Ref. [9]).

**4** The effect of magnetic fields When a magnetic field **B** is applied along the growth direction ([001], which we take to be the z-axis), the lines in the spectra split and become circularly polarised (Fig. 1). For this field direction the optically active states  $|m_{\rm J}, m_{\rm s}\rangle$  for HH excitons are  $|3/2, -1/2\rangle$  and  $|-3/2, 1/2\rangle$ , where  $m_{\rm J}$  and  $m_{\rm s}$  are, respectively, the magnetic quantum numbers for the hole and the electron. The field-induced energy splitting between these states is linear in **B** and can be characterised by a parameter  $g_{\rm exc}$ , where  $E_{\sigma_+} - E_{\sigma_-} = g_{\rm exc}\mu_{\rm B}B$ . Here  $E_{\sigma_+}$  and  $E_{\sigma_-}$  are the photon energies for the  $\sigma_+$  and  $\sigma_-$  transitions and  $\mu_{\rm B}$  is the Bohr magneton.

At first sight, one would expect  $g_{\text{exc}} = g_{\text{HH}} - g_{\text{e}}$ , where  $g_{\text{HH}}$  and  $g_{\text{e}}$  are, respectively, the heavy hole and electron

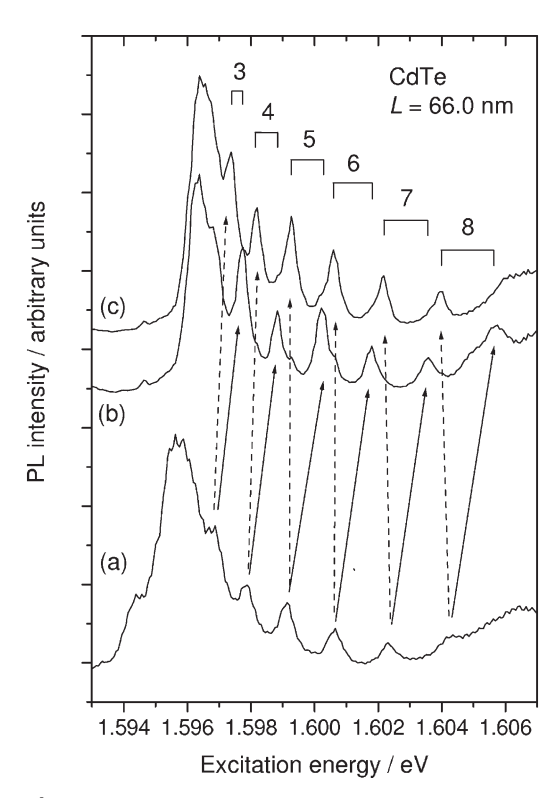


**Figure 1** PLE spectrum obtained by monitoring the intensity of bound exciton luminescence at 3 K from a CdTe quantum well of width 66.0 nm. Trace (a) is for zero magnetic field and traces (b) and (c) are for a field of 5 T directed along the sample growth axis. The light paths were also along the growth axis and traces (b) and (c) are for  $\sigma_-$  and  $\sigma_+$  polarisation of the excitation beam. The arrows indicate the field-induced energy splittings for the transitions with the values of N shown at the top.

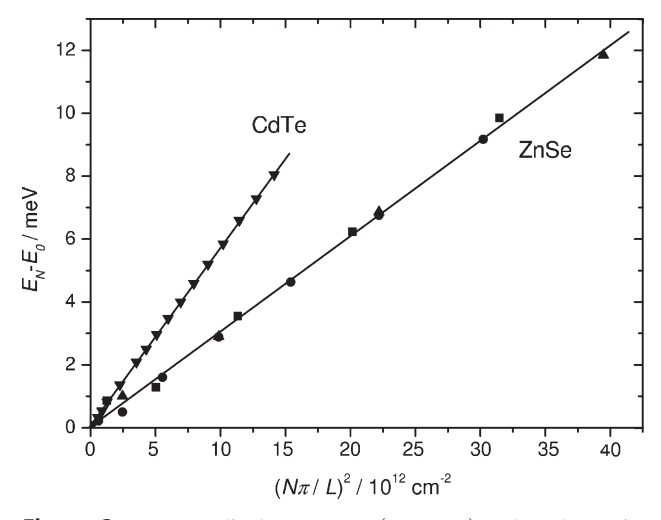


**Figure 2** Energy displacements  $(E_{\rm N}-E_0)$  plotted against  $(N\pi/L)^2$  for a CdTe well with width 167.1 nm (filled inverted triangles) and for three ZnSe wells of widths 20.7 nm (triangles), 29.4 nm (squares) and 43.7 nm (circles).

15213951, 2010, 6, Downloaded from https://onlinelibrary.wiley.com/doi/10.1002/pssb.200983167 by Egyptian National Sti. Network (Enstinet), Wiley Online Library on [12.032023]. See the Terms and Conditions (https://onlinelibrary.wiley.com/term/term).

and-conditions) on Wiley Online Library for rules of use; OA articles are governed by the applicable Creative Common

1521 3951, 2010, 6, Downloaded from https://onlinelibrary.wiley.com/doi/10.1002/pssb.200983167 by Egyptian National Sti. Network (Enstinet), Wiley Online Library on [12.03/2023]. See the Termu ) on Wiley Online Library for rules of use; OA articles are governed by the applicable Creative Common

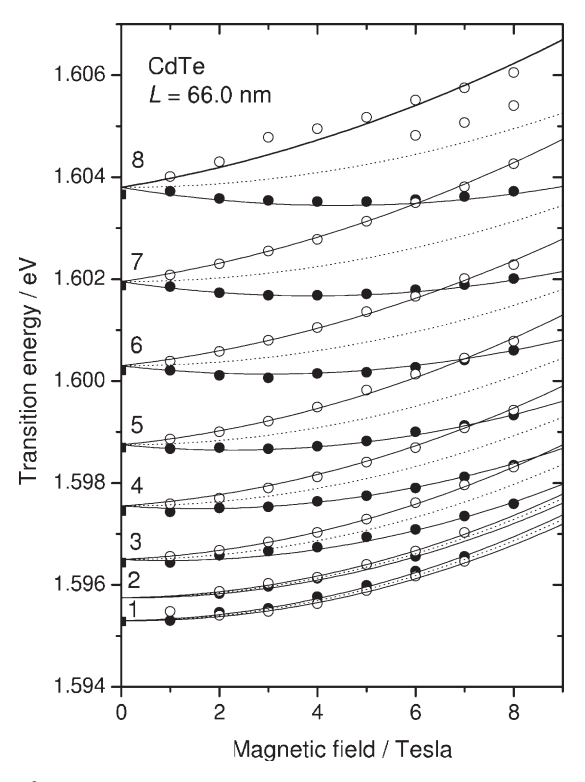
g-values for this field direction, and that, for a given specimen,  $g_{\rm exc}$  would be the same for all values of N. However, it is clear from the experimental data in Fig. 1 that this is not so. The magnitudes of the field-induced splittings, and hence the values of  $g_{\rm exc}$ , increase markedly as the translational quantisation index N gets larger.

These increases in the Zeeman splittings can be seen in more detail in Fig. 3, where the continuous lines are of the form:

$$E = E_{\rm N} + DB^2 \pm \frac{g_{\rm exc}\mu_{\rm B}B}{2}.$$
 (2)

Here, for a given specimen,  $E_N$  and  $g_{\rm exc}$  are functions of N. The term  $DB^2$  represents the diamagnetic shift of the corresponding transition. It is also apparent from Fig. 3 that, in contrast to the values of  $g_{\rm exc}$ , the diamagnetic shifts (which determine the upwards curvatures of the continuous and dotted lines) decrease as N increases. For a given specimen, the parameter D is thus also a function of N. These changes in the paramagnetism and diamagnetism are seen below to be the result of motion-induced mixing of the exciton states.

The values of  $g_{\text{exc}}$  for a series of quantum wells of different widths (but with near-identical strain) are shown in



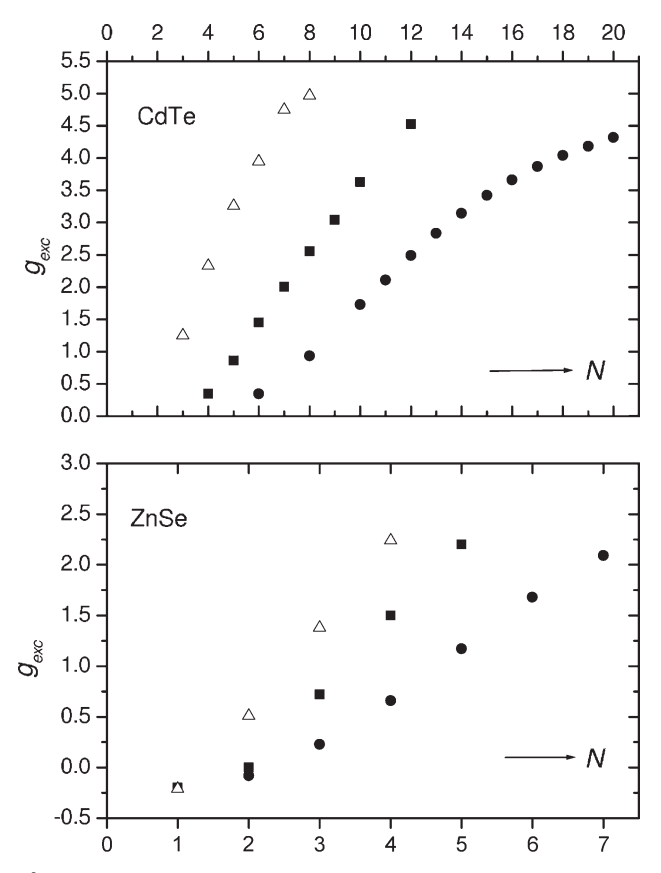
**Figure 3** Transition energies at 3 K for excitons in a CdTe well of width 66.0 nm as functions of a magnetic field applied along the growth direction. Open and filled circles are for  $\sigma_-$  and  $\sigma_+$  polarisations, respectively. The continuous lines are of the form of Eq. (2). The values of N for each transition are indicated at the left of the diagram. The broken lines are the average energies for each value of N and show decreasing curvature as N gets larger.

Fig. 4. As the well width is increased, a larger value of N is required to produce a given value of  $g_{\rm exc}$  and it becomes clear that what matters is not the value of N but the value of  $K_z$ , given by  $N\pi/L$ . When the values of  $g_{\rm exc}$  are plotted against  $K_z$  they are found, for a given material and a given strain in the well, to lie on common curves, as shown in Fig. 5. We deduce therefore that there is a  $K_z$ -dependent contribution to  $g_{\rm exc}$  and write:

$$g_{\rm exc} = g_{\rm HH} - g_{\rm e} + g(\mathbf{K}_z).$$

Similarly, when the values of the diamagnetic parameter D are plotted against  $K_z$  for a series of wells of a given material and strain, they also lie on a common curve (Fig. 6). When the magnetic field is at an angle  $\theta$  to the growth axis, the g-value for a heavy hole is expected to be  $g_{\rm HH}\cos\theta$  [10], whilst that of the electron is expected to be approximately independent of  $\theta$ . Figure 7 shows the experimental values of  $g_{\rm exc}$  as a function of  $\theta$ . We find that we can write:

$$g_{\text{exc}} = -g_{\text{e}} + g_{\text{HH}} \cos \theta + g(\mathbf{K}_z) \cos \theta. \tag{3}$$



**Figure 4** Exciton *g*-values as functions of *N* for quantum wells of different widths for CdTe (upper panel) and for ZnSe (lower panel). For CdTe open triangles, filled squares and filled circles represent well widths of 66.0, 110.0 and 167.1 nm, respectively, whilst for ZnSe they represent in turn widths of 20.7, 29.4 and 43.7 nm. For each material the strain contribution *S* to the energy splitting between LH and HH states is approximately the same in all samples (S = 12-14 meV for CdTe, S = 13 meV for ZnSe).

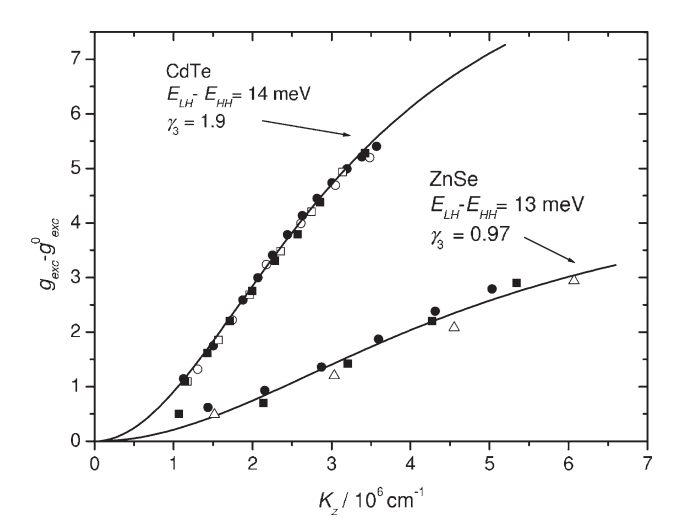


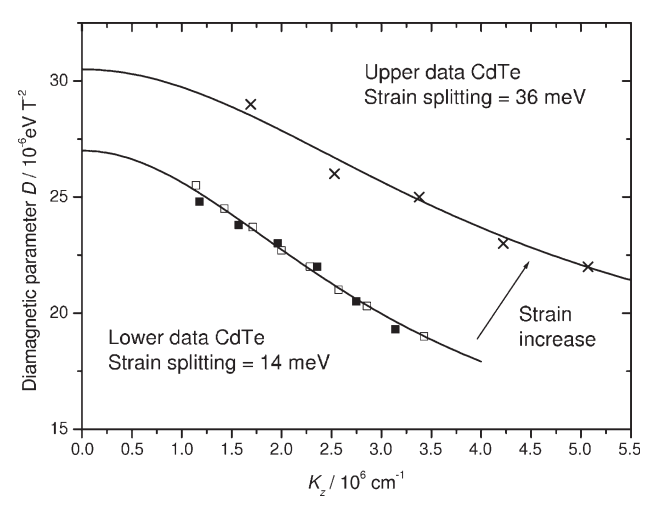
**Figure 5** Exciton *g*-values (relative to their extrapolated values at  $K_z = 0$ ) as functions of the translational wavevector  $K_z$  for CdTe and ZnSe. For each material the strain contribution *S* to the energy splitting between LH and HH states is approximately the same in all samples (S = 14 meV for CdTe and S = 13 meV for ZnSe). For CdTe filled squares, open squares, open circles and filled circles represent well widths of 80.0, 110.0, 144.2 and 167.1 nm, respectively, whilst for ZnSe open triangles, filled squares and filled circles represent in turn well widths of 20.7, 29.4 and 43.7 nm. The continuous lines are those obtained from the model described in the text.

When  $\theta=90^\circ$ , the exciton g-values thus become equal in magnitude to that of an electron (for CdTe,  $g_e\approx-1.6$  [11–14] and for ZnSe,  $g_e\approx1.1$  [15–17]). It is important to note that the exciton's translational motion remains quantised along the growth axis, even though the magnetic field is applied in a different direction.

**5 The motion-induced mixing process** The origin of the  $K_z$ -dependent changes in the magnetic properties is motion-induced mixing between the 1S-like exciton HH ground state and higher lying hydrogenic envelope states. The mixing is due to the presence of terms in the valence band dispersion curve which result in it not being possible to separate the CoM motion and the internal motion (a full discussion of this will be given elsewhere [18]). The relation between energy and wavevector for the valence band can be described by the Luttinger Hamiltonian [19], as follows:

$$-H^{(v)}(\mathbf{k}) = \left(\gamma_1 + \frac{5}{2}\gamma_2\right) \frac{\hbar^2 k^2}{2m_0} - 2\mu_{\rm B}\kappa \mathbf{J} \cdot \mathbf{B}$$
$$-\gamma_2 \frac{\hbar^2}{m_0} (k_x^2 J_x^2 + k_y^2 J_y^2 + k_z^2 J_z^2)$$
$$-2\gamma_3 \frac{\hbar^2}{m_0} (\{k_x k_y\} \{J_x J_y\} + \text{cycl.perm.}),$$
 (4)

where k is the wavevector of the hole and  $\{J_xJ_y\} = (1/2)(J_xJ_y + J_yJ_x)$ , etc. The directions x, y, z refer to the crystal [100], [010] and [001] axes. The quantities  $\gamma_1$ ,  $\gamma_2$ ,  $\gamma_3$  and  $\kappa$  are the (dimensionless) Luttinger parameters and  $m_0$  is the electron rest mass. In Eq. (4) we have omitted the



15213951, 2010, 6, Downloaded from https://onlinelibrary.wiley.com/doi/10.1002/pssb.200983167 by Egyptian National Sti. Network (Enstinet), Wiley Online Library on [12.03/2023]. See the Terms and Conditions (https://online.com/doi/10.1002/pssb.200983167 by Egyptian National Sti. Network (Enstinet), Wiley Online Library on [12.03/2023]. See the Terms and Conditions (https://online.com/doi/10.1002/pssb.200983167 by Egyptian National Sti. Network (Enstinet), Wiley Online Library on [12.03/2023]. See the Terms and Conditions (https://online.com/doi/10.1002/pssb.200983167 by Egyptian National Sti. Network (Enstinet), Wiley Online Library on [12.03/2023]. See the Terms and Conditions (https://online.com/doi/10.1002/pssb.200983167 by Egyptian National Sti. Network (Enstinet), Wiley Online Library on [12.03/2023]. See the Terms and Conditions (https://online.com/doi/10.1002/pssb.200983167 by Egyptian National Sti. Network (Enstinet), Wiley Online Library on [12.03/2023]. See the Terms and Conditions (https://online.com/doi/10.1002/pssb.200983167 by Egyptian National Sti. Network (Enstinet), Wiley Online Library on [12.03/2023]. See the Terms and Conditions (https://online.com/doi/10.1002/pssb.200983167 by Egyptian National Sti. Network (Enstinet), Wiley Online Library on [12.03/2023]. See the Terms and Conditions (https://online.com/doi/10.1002/pssb.200983167 by Egyptian National Sti. Network (https://online.com/doi/10.1002/pssb.200983167 by Egyptian National Nat

conditions) on Wiley Online Library for rules of use; OA articles are governed by the applicable Creative Comm

**Figure 6** The diamagnetic parameter D as a function of  $K_z$  for CdTe wells with a LH–HH strain splitting of S=14 meV (lower trace) and S=36 meV (upper trace). The well widths are 36.5 nm (filled triangles), 80.0 nm (filled squares) and 110.0 nm (open squares). The continuous curves are those obtained from the model in the text.

electron-hole exchange interaction, which is small (less than 1 meV) and does not affect the Zeeman splittings for  $\theta = 0$ . We have also omitted small terms involving  $B_x J_x^3$ , etc. so that  $g_{\rm HH} \approx -6\kappa$ .

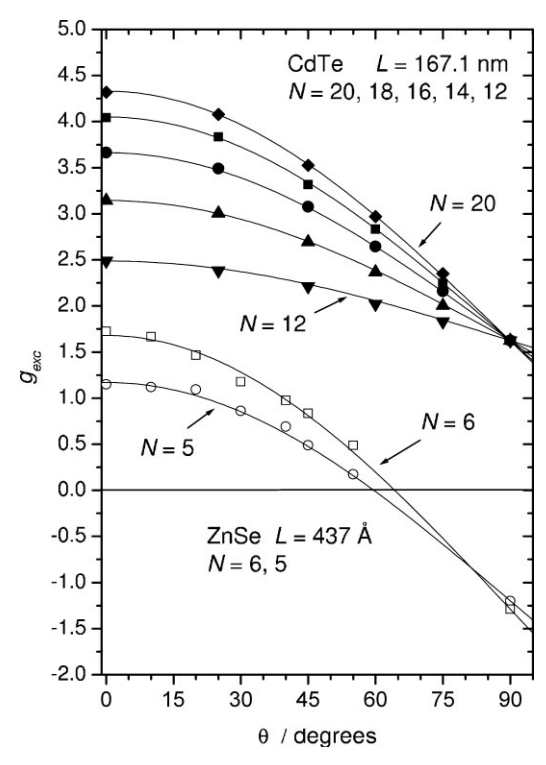


**Figure 7** Dependence of exciton *g*-values on the direction of the magnetic field relative to the growth axis for transitions with various values of the quantisation index N, for quantum wells of widths 167.1 nm (CdTe, upper set) and of 43.7 nm (ZnSe (lower trace). The *g*-values for each sample converge to -1 times the electron *g*-value when  $\theta = 90^{\circ}$ .

15213951, 2010, 6, Downloaded from https://onlinelibrary.wiely.com/doi/10.002/pssb.200983167 by Egyptian National St. Network (Enstinet), Wiley Online Library on [12.032023], See the Terms and Conditions (thtps://onlinelibrary.wiely.com/terms-and-conditions) on Wiley Online Library for rules of use; OA articles are governed by the applicable Ceravite Commons.

To describe excitons in the CoM approximation, one replaces k by  $(-p/\hbar + eA/\hbar + \beta K)$  [20–22]. Here p is the momentum operator for the electron within the exciton (equal to minus that of the hole). The parameter  $\beta = m_{\rm HH}/(m_{\rm e} + m_{\rm HH})$  represents the fraction of the momentum carried by the heavy hole (of effective mass  $m_{\rm HH}$ ,  $m_{\rm e}$  being the effective mass of the electron). The vector potential A (for B along z) is given [20–22] by  $(1/2)B \times r$ , where r is the electron–hole separation. For (001) wells with magnetic fields at an angle  $\theta$  to the growth direction, the terms in the extended Hamiltonian which cause changes in the exciton g-value [2] are those which involve  $\gamma_3$ . These terms become:

$$H_{\pm} = \pm \frac{\gamma_3 \hbar \beta}{2m_0} \left( p_{\pm} \mp i r_{\pm} \frac{eB \cos \theta}{2} \right)$$

$$\times (J_{\mp} J_z + J_z J_{\mp}) \mathbf{K}_z$$
(5)

where  $p_{\pm}=p_x\pm ip_y$ ,  $p_x=-i\hbar\partial/\partial x$ , etc. and  $r_{\pm}=x\pm iy$ . The parts of  $H_{\pm}$  which involve  $p_{\pm}$  and  $r_{\pm}$  mix the 1S state with nP states, whilst those parts which involve  $J_{+}$  and  $J_{-}$  cause it to be light hole states of nP form that are mixed with the 1S heavy hole ground state. The energy of these LH states relative to the HH states depends on the amount of strain. The extent of the mixing and hence the magnitude of the changes in the magnetic properties therefore depend on the strain in the quantum well.

The changes in the magnetic properties can be calculated by using perturbation theory. To illustrate this, we consider mixing between the 1S and 2P states. The 1S HH ground states with  $m_{\rm s}=\mp 1/2$ ,  $m_{\rm J}=\pm 3/2$  are mixed with 2P states with  $m_{\rm s}=\mp 1/2$ ,  $m_{\rm J}=\pm 1/2$ ,  $m_{\rm I}=\pm 1$ , where  $m_{\rm I}$  is the orbital quantum number. The matrix elements involved are of the form  $|M_{\pm}|=(a\pm bB\cos\theta)K_z$ , respectively, where a and b are both proportional to  $\gamma_3$  (see Eq. 5 of Ref. [2]). The energies of the ground states are then depressed by amounts  $(a\pm bB\cos\theta)^2K_z^2/\Delta E_2$ , where  $\Delta E_2$  is the energy difference between the unperturbed 2P LH and 1S HH state, given by:

$$\Delta E_2 = \frac{3R}{4} + S + \hbar^2 \left( \frac{1}{2M_{\rm LH}} - \frac{1}{2M_{\rm HH}} \right) K_z^2.$$
 (6)

The cross terms (linear in *B*) lead to contributions to the energy changes which are of opposite signs for the  $m_{\rm s}=\mp 1/2,\,m_{\rm J}=\pm 3/2$  states; in other words, they lead to a contribution to the Zeeman splitting and therefore to  $g_{\rm exc}$ . The contributions to the *g*-value are [2] of the form:

$$\delta g = \frac{2ab\mathbf{K}_z^2}{\mu_{\rm B}\Delta E_2} = \left(\frac{24\gamma_3^2\hbar^2\beta^2\cos\theta}{m_0}\right) \left(\frac{v_2w_2}{\Delta E_2}\right) \mathbf{K}_z^2,\tag{7}$$

where  $v_2 = -\langle 2P, p_x | \partial/\partial x | 1S \rangle a_{\rm exc} = 0.279$  and  $w_2 = \langle nP, p_x | x | 1S \rangle a_{\rm exc}^{-1} = 0.745$ . In addition, the terms which are quadratic in *B* lead to  $K_z$ -dependent decreases in the diamagnetic shifts. There are contributions to the diamagnetic parameter *D* which, for  $\theta = 0$ , are [2] of the

orm.

$$\delta D_0(\mathbf{K}_z) = -\frac{b^2 \mathbf{K}_z^2}{\Delta E_2}$$

$$= -\frac{3}{2} \left(\frac{\gamma_3 \beta \hbar e a_{\text{exc}}}{m_0}\right)^2 \left(\frac{w_2^2}{\Delta E_2}\right) \mathbf{K}_z^2. \tag{8}$$

There are similar contributions to  $g_{\rm exc}$  and to D from all nP states, including P-like states in the continuum [2] and these have to be integrated over all such excited states. The results of such calculations are shown by the curves in Figs. 5 and 6. The trend towards saturation in these curves at high values of the translational wavevector is caused by the presence of  $K_z$  in the energy denominator  $\Delta E_2$ .

We note here that the wavevectors which we consider are less than  $10^7 \, \text{cm}^{-1}$ , compared with the zone boundary wavevectors of order  $10^8 \, \text{cm}^{-1}$ , so we assume that departures of the valence band from Eq. (4) can be ignored.

**6 Discussion** The model outlined above leads to excellent quantitative agreement with the experimental data for the  $K_7$ -dependence of the exciton g-values for both CdTe and ZnSe. This is illustrated by the calculated curves for  $g_{\rm exc}$ in Fig. 5, which are obtained using published values for the following parameters: for CdTe,  $\gamma_1 = 4.7 \pm 0.3$ ,  $\gamma_2 = 1.45 \pm 0.15$  [23],  $m_e = 0.09m_0$  and R = 11 meV [24] and for ZnSe,  $\gamma_1 = 2.45$ ,  $\gamma_2 = 0.61$  [25]  $m_e = 0.145m_0$  [26] and  $R=20\,\mathrm{meV}$  [26]. The variation of  $g_\mathrm{exc}$  with  $K_z$  depends critically on  $\gamma_3$  and to fit the data we use  $\gamma_3 = 1.9$  for CdTe and  $\gamma_3 = 0.97$  for ZnSe. These values are close to those obtained by other methods ( $\gamma_3 = 1.9$  [23] for CdTe and  $\gamma_3 = 1.11$  for ZnSe [25]). The strain splitting S is sample dependent and can be measured directly from the spectra or calculated from the known sample parameters. To fit the data in Fig. 5, we have used the values of  $g_{\rm HH} = -2.4$  (CdTe) and  $g_{\rm HH} = 0.4$  (ZnSe); the choice of these values determines the intercept at  $K_z = 0$  and thus slides the calculated curve as a whole in the vertical direction (there is evidence [2] that the values of  $g_{\rm HH}$  are strain-dependent).

The model also accounts well for the angular dependence of the *g*-values (Fig. 7), since the mixing causes changes to  $g_{\rm exc}$  which contain the factor  $\cos\theta$  (Eq. 7).

The calculated variation in the diamagnetic parameter D is shown in Fig. 6. The calculated curve depends on the value chosen for  $a_{\rm exc}$  (see Eq. 8) and, for CdTe,  $a_{\rm exc}=7.2\,{\rm nm}$  provides an excellent fit [2]. For ZnSe, the dependence of the diamagnetic parameter on  $K_z$  is much less pronounced, since the expected value of about 3.5 nm for  $a_{\rm exc}$  is much smaller than for CdTe.

The relevance of strain, which enters via the term S in Eq. (6), is illustrated in Fig. 8. This shows the effect on the g-values of increasing the strain by growth on a different substrate. The model accounts well for the observed changes, with only a slight change in  $\gamma_3$ . It also accounts well for the accompanying changes in the diamagnetic parameter, as shown in Fig. 6. Cases in which the strain splitting is such that

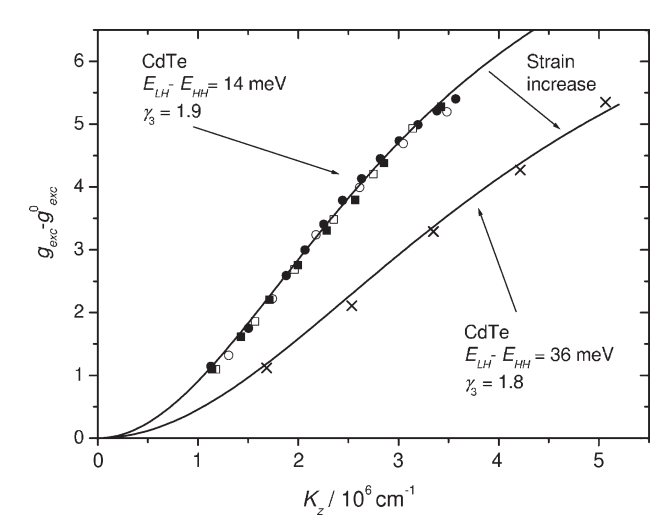


**Figure 8** The effect on the exciton g-values of increasing the strain contribution to the LH–HH splitting. The crosses represent data for a CdTe well of width 37.0 nm and with  $S = 36 \,\mathrm{meV}$ . The other symbols (for  $S = 14 \,\mathrm{meV}$ ) have the same meaning as in Fig. 5. The continuous lines are calculated as described in the text.

light hole excitons lie lower in energy than heavy hole excitons are more difficult to treat. In this case, the 1S lighthole exciton ground state will be mixed with heavy hole states of nP character. However, problems arise since the light-hole dispersion curve rises more quickly than that of the heavy hole as  $K_z$  gets larger and the perturbation theory becomes inappropriate. There is, however, clear experimental evidence, for the case of ZnTe quantum wells grown with ZnMgTe barriers [27], that the magnetic properties of the excitons have strong dependences on the translational wavevectors. However, discussion of this case lies beyond the scope of the present paper. More generally, it is the presence of a large energy splitting between the HH ground state and the excited nP LH states which make possible the present simple calculation. This is not the case for unstrained GaAs and for the oppositely strained ZnTe.

A final comment concerns the fact that we have used quantum wells to study the dependence of the exciton magnetism on kinetic energy. The mixing process will, however, apply equally to excitons in motion in a bulk material: the use of quantum wells has simply been an expedient which has made the optical studies possible.

**7 Conclusions** The experiments described above show clearly that the magnetic properties of excitons are affected strongly as they acquire kinetic energy. In the center of mass approximation, the origin of the effect is motion-induced mixing between the 1S exciton ground state and excited states of nP form. The mixing is due to the  $\gamma_3$  term in the valence band dispersion curve. In the presence of such terms, the CoM motion and the internal motion of the particles within the exciton cannot be separated. Both for CdTe and for ZnSe, calculations based on this mixing process have led to excellent quantitative agreement with the

observed motion-induced changes of the magnetic moments and of the diamagnetic shifts. For the (001) quantum wells studied above, these changes are dependent primarily on the value of  $\gamma_3$  and the values chosen to fit the experimental data are in excellent agreement with those determined by other means. The success of the model thus provides convincing evidence that the structure of excitons in zinc-blende semiconductors is significantly affected as the excitons acquire motion.

**Acknowledgements** We are grateful for support from the EPSRC(UK) (project EP/E025412), the Royal Society, the RFBR, the Presidium RAS, the EU within the European Regional Development Fund (Innovative Economy grant POIG.01.01.02-00-008/08), the Ministry of Science and Higher Education (Poland) through grant N515 015 32/0997 and the German Research Foundation DFG within project Ho1388/28 (A. Gust).

## References

- [1] J. J. Davies, D. Wolverson, V. P. Kochereshko, A. V. Platonov, R. T. Cox, J. Cibert, H. Mariette, C. Bodin, C. Gourgon, E. V. Ubyivovk, Yu. P. Efimov, and S. A. Eliseev, Phys. Rev. Lett. 97, 187403 (2006).
- [2] L. C. Smith, J. J. Davies, D. Wolverson, S. Crampin, R. T. Cox, J. Cibert, H. Mariette, V. P. Kochereshko, M. Wiater, G. Karczewski, and T. Wojtowicz, Phys. Rev. B 78, 085204 (2008).
- [3] V. P. Kochereshko, L. C. Smith, J. J. Davies, R. T. Cox, A. Platonov, D. Wolverson, H. Boukari, H. Mariette, J. Cibert, M. Wiater, T. Wojtowicz, and G. Karczewski, Phys. Status Solidi B 245, 1059 (2008).
- [4] V. P. Kochereshko, A. Platonov, D. Loginov, J. J. Davies, D. Wolverson, L. C. Smith, H. Boukari, R. T. Cox, J. Cibert, and H. Mariette, Semicond. Sci. Technol. 23, 114011 (2008).
- [5] J. J. Davies, L. C. Smith, D. Wolverson, H. Boukari, R. T. Cox, H. Mariette, J. Cibert, and V. P. Kochereshko, J. Korean Phys. Soc. 53, 2803 (2008).
- [6] J. J. Davies, L. C. Smith, D. Wolverson, A. Gust, C. Kruse, D. Hommel, and V. P. Kochereshko, Phys. Rev. B 81, 085208 (2010).
- [7] E. L. Ivchenko and G. Pikus, Superlattices and Other Microstructures (Springer-Verlag, Berlin, 1995).
- [8] E. L. Ivchenko, Semiconductor Nanostructures (Alpha Science International, Harrow, UK, 2005).
- [9] S. Schumacher, G. Czycholl, F. Jahnke, I. Kudyk, H. I. Rückmann, J. Gutowski, A. Gust, G. Alexe, and D. Hommel, Phys. Rev. B 70, 235340 (2004).
- [10] J. L. Patel, J. E. Nicholls, and J. J. Davies, J. Phys. C (Solid State Phys.) 14, 1339 (1981).
- [11] M. V. Alekseenko and A. I. Veinger, Sov. Phys. Semicond. 8, 143 (1974).
- [12] M. Willatzen, M. Cardona, and N. E. Christensen, Phys. Rev. B 51, 17992 (1995).
- [13] A. A. Sirenko, T. Ruf, M. Cardona, D. R. Yakovlev, W. Ossau, A. Waag, and G. Landwehr, Phys. Rev. B 56, 2114 (1997).
- [14] S. Tsoi, I. Miotkowski, S. Rodrigeuz, A. K. Ramdas, H. Alawadhi, and T. M. Pekarek, Phys. Rev. B 69, 035209 (2004).
- [15] J. E. Nicholls, J. J. Davies, N. R. J. Poolton, R. Mach, and G. O. Müller, J. Phys. C: Solid State Phys. 18, 455 (1985).

15213951, 2010, 6, Downloaded from https://onlinelibrary.wiely.com/doi/10.1002/pssb.20983167 by Egyptian National Sti. Network (Ensiret), Wiley Online Library on [12.032023]. See the Terms and Conditions (thps://onlinelibrary.wiely.com/terms-and-conditions) on Wiley Online Library for rules of use; OA articles are governed by the applicable Ceretive Common

1521 3951, 2010, 6, Downloaded from https://onlinelibrary.wiley.com/doi/10.1002/pssb.200983167 by Egyptian National Sti. Network (Enstinet), Wiley Online Library on [12.03/2023]. See the Terms and-conditions) on Wiley Online Library for rules of use; OA articles are governed by the applicable Creative Commons

- [16] D. J. Dunstan, J. E. Nicholls, B. C. Cavenett, and J. J. Davies,J. Phys. C: Solid State Phys. 13, 6409 (1980).
- [17] J. J. Davies, D. Wolverson, I. J. Griffin, O. Z. Karimov, C. L. Orange, D. Hommel, and M. Behringer, Phys. Rev. B 62, 10329 (2000).
- [18] V. P. Kochereshko, to be published.
- [19] J. M. Luttinger, Phys. Rev. 102, 1030 (1956).
- [20] J. O. Dimmock, in: Semiconductors and Semimetals, edited by R. K. Willardson and A. C. Beer (Academic, New York, 1967), Vol. 3, p. 259.
- [21] M. Altarelli and N. O. Lipari, Phys. Rev. 7, 3798 (1973).
- [22] K. Cho, S. Suga, W. Deybrodt, and F. Willman, Phys. Rev. B 11, 1512 (1975).

- [23] L. S. Dang, G. Neu, and R. Romestain, Solid State Commun. 44, 1187 (1982).
- [24] H. Mariette, F. Dal'bo, N. Magnea, G. Lentz, and H. Tuffigo, Phys. Rev. B 38, 12443 (1988).
- [25] H. W. Hölscher, A. Nöthe, and Ch. Uihlein, Phys. Rev. B 31, 2379 (1985).
- [26] J. Gutowski, K. Sebald, and T. Voss, in: Landolt-Börnstein, Numerical Data and Functional Relationships in Science and Technology, Group III: Condensed Matter, Vol. 44: Semiconductors, Subvolume B: New Data and Updates for II-VI Compounds (Springer-Verlag, Berlin, 2008).
- [27] L. C. Smith, J. J. Davies, D. Wolverson, V. P. Kochereshko, H. Boukari, J. Cibert, and H. Mariette, to be published.